

pubs.acs.org/acsapm Article

Role of Material Composition in Photothermal Actuation of DASA-Based Polymers

Miranda M. Sroda, Jaejun Lee, Younghoon Kwon, Friedrich Stricker, Minwook Park, Megan T. Valentine,* and Javier Read de Alaniz*



ACCESS I

Cite This: ACS Appl. Polym. Mater. 2022, 4, 141-149

Metrics & More



Article Recommendations

Decreased actuation performance "click" platform performance

Low T_g
Low Might on light on light on modulus modulus

ABSTRACT: We investigate the influence of the host matrix on the photothermally driven actuation performance of negatively photochromic, donor—acceptor Stenhouse adduct (DASA)-based polymers. Using a modular Diels—Alder "click" platform, we designed polymeric materials with varying DASA incorporation and investigated the relationships between the material composition and the resulting physical, mechanical, and photoswitching properties. We demonstrate that increasing the DASA concentration in polymer conjugates has a dramatic effect on the material's physical and mechanical properties, such as the glass transition temperature $(T_{\rm g})$ and elastic modulus, as well as the photoswitching properties, which are found to be highly dependent on $T_{\rm g}$. We establish using a simple photoresponsive bilayer that actuation performance is controlled by the bilayer stiffness rather than the photochrome incorporation of DASA. Finally, we report and compare the light-induced property changes in $T_{\rm g}$ and the elastic modulus between the materials comprising the open or closed forms of DASAs. Our results demonstrate the importance of designing a material that is stiff enough to provide the mechanical strength required for actuation under load, but soft enough to reversibly switch at the operational temperature and provide key considerations for the development of application-geared photoswitchable materials.

KEYWORDS: donor-acceptor Stenhouse adducts, photothermal actuation, photo-induced property changes, negative photochromism, glass transition temperature

■ INTRODUCTION

Light-responsive materials have garnered significant attention for their abilities to form soft actuators, for example, as locomotive robots, 1-5 artificial muscles, 6,7 grippers, 8,9 and oscillators. 10,11 Light offers numerous advantages: it is readily available by solar or artificial sources, does not require physical contact for delivery of power or signals, and has noninteracting internal degrees of freedom (wavelength, mode, and polarization). In one straightforward realization, lightresponsive bilayer actuators exploit the differential volumetric expansion between two material layers to generate motion and mechanical work under light stimulus via combined photothermal and photomechanical mechanisms. 9,11-13 Under illumination, the photoactive layer is rapidly heated and the material property mismatch between the two layers causes the development of mechanical stress at the interface, which leads to rapid and easily observed bending of the cantilever, with an amplitude that is highly sensitive to the bilayer stiffness. The

stiffness in turn depends on the glass transition temperature $T_{\rm g}$ and elastic modulus. 14,15

Supporting Information

To boost the actuation potential of the active layer, additives including carbon-based materials, ^{16,17} gold nanoparticles, ^{18,19} and organic dyes²⁰ are often added to enhance the conversion of light energy into heat. Among additives, photoswitches offer particular benefits in energy conversion, tunability, and high compatibility in soft materials. ^{21,22} A visible-light-responsive bilayer actuator system driven by the photothermal properties of a unique molecular photoswitch: donor—acceptor Stenhouse adduct (DASA; Figure 1a) was recently developed by

Received: August 30, 2021 Accepted: December 23, 2021 Published: January 5, 2022





a) Negatively photochromic donor-acceptor Stenhouse adducts (DASAs) photoswitching

b) Schematic and chemical structure of modular approach to a range of DASA-based materials

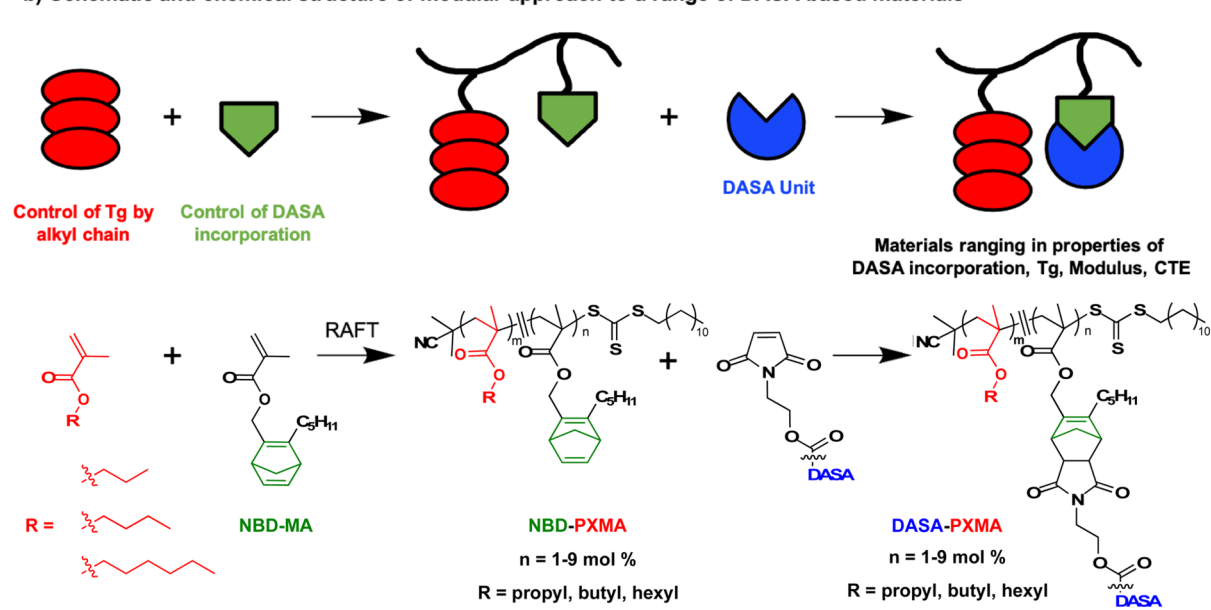


Figure 1. (a) Upon irradiation with visible light, DASAs undergo a conformational change from a highly colored, open-form to a colorless, closed-form. (b) Schematic and chemical structure of the modular cascading Diels—Alder "click" approach used to synthesize a range of DASA-based materials that vary in incorporation of the photoresponsive unit and glass transition temperature.

our groups. This system demonstrates rapid and repeatable actuation capabilities, and the ability of the cantilever to lift more than ten times its own weight.²³ Moreover, by leveraging the negative photochromism of DASAs, in which the photoproduct absorption shifts to a shorter wavelength with respect to the reactant absorption (blue shift) and thus does not absorb the exciting light, we demonstrated tunable actuation performance of DASA—poly (hexyl methacrylate) (PHMA) under constant light intensity.

Further use of DASA photoswitches in soft material applications requires a deeper understanding of the effects of DASAs on the physical and mechanical properties of materials so that the material composition can be optimally designed. DASAs are known to be highly sensitive to their local environment, 24-26 and while the complicated and concentration-dependent mechanisms of DASA switching in solution have gained considerable attention, ^{27–31} the effects of DASA incorporation on polymeric material properties including the glass transition temperature (T_g) , coefficient of thermal expansion (CTE), and elastic modulus have not been thoroughly explored. Prior studies have shown that photoswitching of DASAs^{32,33} and other photochromes^{34–37} is highly influenced by the glass transition temperature as thermal reversion is inhibited in a glassy matrix that possesses a high modulus. We anticipate that there will be an inherent trade-off between having a system that is stiff enough to actuate and perform work, but soft enough to enable photoswitching at the operational temperature.

In order to establish the relationships between material composition and actuation performance, we developed robust and scalable synthetic methods to access a range of DASAbased materials. Specifically, using a modular Diels-Alder "click" approach, ^{23,38} shown in Figure 1b, we elucidate the role of T_{σ} and elastic modulus in photothermal actuation by tuning the polymer host matrix and DASA incorporation. By synthesizing materials with increasing DASA content and constant T_g, we can decouple the effects of DASA incorporation and $T_{\rm g}$ on material performance metrics. We show that the effect of the performance of actuation is directly related to the material stiffness, which depends on the polymer host matrix, rather than photochrome incorporation of DASA alone. However, in a given polymer host matrix, increasing the DASA incorporation increases the elastic modulus and T_g of polymer conjugates, leading to an improved actuation performance. The increase in glass transition temperature with increasing DASA incorporation also affects the forward and backward switching kinetics. The forward kinetics becomes slow with increasing $T_{\rm g}$, while thermal reversion is essentially shut down at temperatures below $T_{\rm g}$. When materials are held at a temperature above T_{gy} regardless of incorporation or comonomers, there is increased recovery.

The molecular origins of these effects likely arise from changes in the molecular volume, polarity, and molecular interactions between isomers and polymer chains as the photoswitches reversibly switch between two different isomers. Understanding how these molecular-level changes allow for

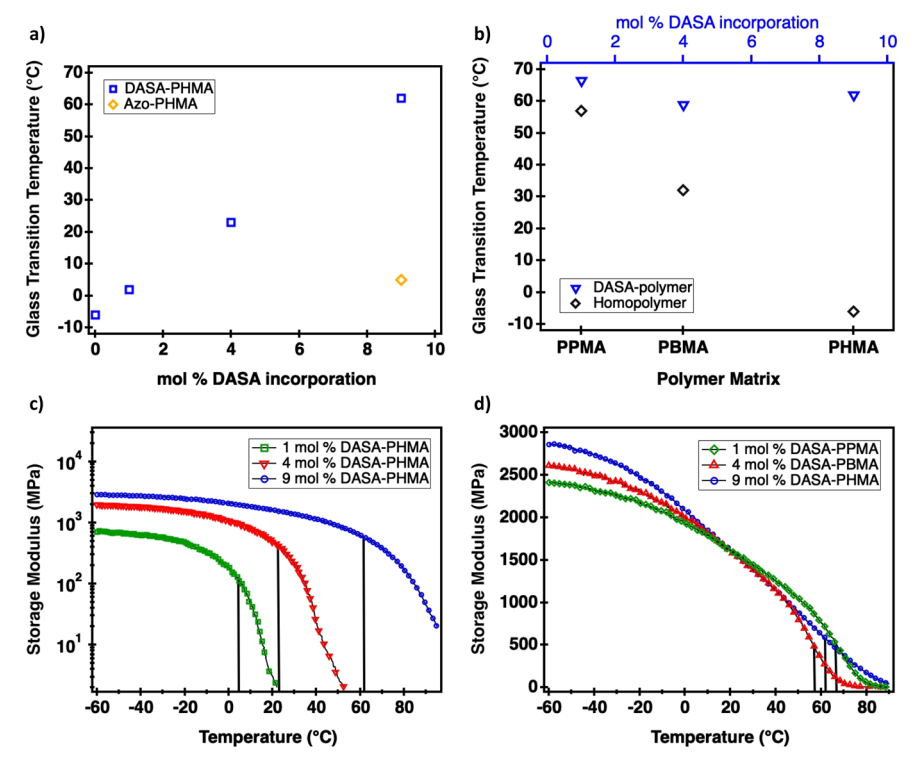


Figure 2. (a) DSC of DASA–PHMA materials shows that $T_{\rm g}$ increases with increasing DASA incorporation. At 9 mol % incorporation of photoswitch, there is a significantly larger increase in $T_{\rm g}$ after functionalization with DASA (blue) compared to azobenzene (Azo). (b) $T_{\rm g}$ of increasing DASA incorporation with different methacrylate comonomers (blue, upper x-axis), and the corresponding methacrylate homopolymers with no DASA showing the increase in $T_{\rm g}$ due to DASA incorporation (black). (c) DMA shows an increase in the elastic modulus of DASA–PHMA with increasing DASA incorporation. (d) By using different methacrylate comonomers, it is possible to obtain materials with varying DASA incorporation and a similar modulus, with vertical lines indicating the similar $T_{\rm g}$ values of each material.

photo-induced mechanical property changes between a photoreactant and a photoproduct would provide an additional handle for actuator design. To better understand the light-induced property changes in $T_{\rm g}$ and modulus, we compare the properties of materials formed from open and closed forms of DASA. We observed a decrease in the modulus and $T_{\rm g}$ upon photoswitching from the highly colored, extended, open form to the colorless, compact closed form, which can be further leveraged in photothermal actuator design.

RESULTS AND DISCUSSION

Synthesis of DASA-Based Materials. To understand how material properties, including the host matrix properties and photochrome incorporation, influence photoswitching, mechanics, and actuation performance, we need robust, modular, scalable methods that enable access to a range of DASA-based materials. Using a modular cascading Diels-Alder "click" approach, we can easily tune the polymer host matrix and incorporation of a photoresponsive unit as shown in Figure 1b. We hypothesized that increasing the concentration of DASA, which acts as a photothermal agent, would increase the actuation performance due to higher heat generation. To test this experimentally, we synthesized copolymers containing PHMA and the functional monomer norbornadiene methacrylate (NBD-MA) using reversible addition fragmentation chain-transfer (RAFT) polymerization. The incorporation of DASA was tuned by varying the equivalence of NBD-MA. Deprotection of the NBD group with tetrazine revealed the cyclopentadiene functional group that spontaneously reacts in situ with the maleimide functionalized DASA photoswitch. The mild and efficient nature of the cascading Diels—Alder chemistry enables facile incorporation of 1, 4, and 9 mol % DASA—PHMA (See Supporting Information Table S1 for incorporation of NBD and DASA based on ¹H NMR spectroscopy). To control the glass transition temperature, the host matrix was tuned by incorporating methacrylates with different alkyl chain lengths, such as hexyl, butyl, or propyl.

Incorporation of DASA was characterized by 1 H NMR spectroscopy, and the molecular weight and polydispersity were characterized by advanced polymer chromatography (APC). Molecular weights of norbornadiene copolymers were targeted to exceed the molecular weight of entanglement of poly (hexyl methacrylate) ($M_{\rm e} = 33~{\rm K}$). The number average molecular weight determined by APC ranged from $M_{\rm n} = 40-70~{\rm K}$, with a dispersity of 1.3–1.7. Using materials designed with varying DASA incorporation and matrix compositions, we next investigated the role of the glass transition temperature in photothermal actuation enabled by DASAs.

Physical and Mechanical Properties of DASA-Based Materials. For each material composition, differential scanning calorimetry (DSC) and dynamic mechanical analysis (DMA) experiments were performed to determine the glass transition temperature. Based on the DSC analysis, 1, 4, and 9 mol % DASA-PHMA conjugates indicated an increase in $T_{\rm g}$ with increasing DASA content, to 2, 23, and 62 °C, respectively, as shown in Figure 2a, as compared to the $T_{\rm g}$ of the PHMA homopolymer, which is -6 °C (Figure S1). To compare the effect of DASA incorporation to that of a well-studied photoswitch, we also synthesized and characterized an

Table 1. Summary of Material Properties of DASA-Based Materials

material	T_g (°C)	modulus ^a (GPa)	$CTE^b(\times 10^{-6}/^{\circ}C)$	temp. c ($^{\circ}$ C)	displacement ^c (mm)
1 mol % DASA-PHMA	2	0.003	142.8 ± 1.4	52.1 ± 3.6	0.65 ± 0.06
4 mol % DASA-PHMA	23	0.495	153.6 ± 0.9	57.9 ± 1.7	1.11 ± 0.06
9 mol % DASA-PHMA	62	1.608	148.4 ± 0.6	62.4 ± 0.9	7.0 ± 0.1
1 mol % DASA-PPMA	67	1.613	134.7 ± 1.1	58.0 ± 0.8	6.8 ± 0.4
4 mol % DASA-PBMA	59	1.604	140.2 ± 0.7	61.7 ± 1.4	6.73 ± 0.08

"Measured at 20 °C by 1 Hz oscillation in the small strain regime. ^bMeasured in the glassy state from -50 °C + $T_{\rm g}$ to -10 °C + $T_{\rm g}$. ^cMeasured at 172 mW/cm².

azobenzene (Azo)-conjugated polymer, 9 mol % Azo–PHMA. The Azo-based material indicated $T_{\rm g}$ = 5 °C, only 11 °C above that of the PHMA homopolymer, in contrast to the equivalent DASA-based material, which indicated $T_{\rm g}$ = 62 °C, an approximately 6-fold larger change (Figure S2). This result highlights the large effect DASA incorporation has on material properties. Presumably, the bulky conjugated groups on DASA increase the $T_{\rm g}$ of the polymer due to restricted segmental dynamics. 41,42

With a better understanding of the effect of increasing DASA incorporation on T_g , we next selected specific comonomers to produce materials with differing DASA content but similar $T_{\rm g}$ and compared their performance. This allowed us to decouple the effects of DASA incorporation and $T_{\rm g}$ on material properties. Materials with a $T_{\rm g}$ of approximately 60 °C were targeted, to facilitate comparisons with the PHMA-based material with the highest incorporation of DASA, 9 mol % DASA-PHMA. To achieve a 1 mol % DASA-based material with a target $T_{\rm g}$ of ~60 °C, we selected copolymers containing propyl methacrylate, for which the homopolymer $T_{\rm g}$ = 57 $^{\circ}$ C (Figure S3). The resulting 1 mol % DASA—PPMA material has a T_{σ} of 67 °C. To achieve a 4 mol % DASA-based material, butyl methacrylate was chosen, for which the homopolymer T_g = 32 °C (Figure S4). The resulting 4 mol % DASA-PBMA material has a $T_{\rm g}$ of 59 °C. While there is a slight variation from the target value among the different compositions, the $T_{\rm g}$ values of all materials were within a narrow range from 59-67°C, enabling quantitative comparisons of materials with an increasing incorporation of DASA and similar T_{φ} as shown in Figure 2b.

With these materials in hand, we determined the mechanical properties of the various material compositions using DMA. Elastic moduli of DASA-PHMA exhibited an increase at all temperatures as shown in Figure 2c. The modulus in the glassy state increased with increasing DASA content. Each DASA-PHMA showed a decrease in the modulus over its T_{σ} and a modulus plateau was not observed due to the relatively low M_n . We found significantly different elastic moduli at 20 °C for DASA-PHMAs, where 1, 4, and 9 mol % DASA-PHMA showed 0.003, 0.495, and 1.608 GPa, respectively. When the materials with increasing incorporation of DASA and similar T_o were compared, we found them to have nearly identical moduli, as shown in Figure 2d, at 20 °C with an average value of 1.609 \pm 0.004 GPa, as measured by 1 Hz oscillation in the small strain regime. We next measured the linear CTE using DMA. We found that DASA-based materials in a glassy state (–50 $^{\circ}\mathrm{C}$ + T_{g} to –10 $^{\circ}\mathrm{C}$ + $T_{\mathrm{g}})$ have similar CTE values (130– 160×10^{-6} /°C) regardless of the DASA incorporation and the matrix, as shown in Figures S5-S15. These values are only based on the glassy region due to the significant creep behavior observed over T_{σ} .

Taken together, our results demonstrate that increasing the DASA incorporation has a significant effect on the $T_{\rm g}$ and modulus, but not the CTE, and that for a given matrix composition, adding DASA increases the material's stiffness as summarized in Table 1. These structure—property relationships can have a profound effect on the ability of the material to bear loads. Through the use of strategic design, we were able to access DASA-materials with a range of mechanical properties. We expect that these properties will be reflected in photoswitching and photoactuation performances as well.

Photoswitching Properties of DASA-Based Materials. DASAs offer the unique advantage of negative photochromism, switching from a highly colored, absorbing open-form to a colorless, non-absorbing closed-form upon irradiation with visible light (Figure 1a). Negative photochromism permits deep penetration of the incident light, allowing photoconversion of the entire sample, and also allows for tunable actuation based on absorbance, where the high absorbing open form has increased photothermally driven actuation, compared to the non-absorbing closed form. 23,43 To investigate the photoswitching kinetics of DASA-based polymer materials and to establish the influence of the DASA content and material T_{φ} we used time-dependent pump-probe UV/vis spectroscopy (for experimental details, see Section 1.2.5 and Section 4 in the Supporting Information). The wavelength of maximum absorbance in all DASA materials was centered at ~648 nm as shown in Figure S16 and was used to monitor the rates of the forward photoswitching and the thermal back reaction. Using a two state model, we can quantify the forward reaction rate under light $(k_{\mathrm{f,light}})$ and effective quantum yield (φ_{eff}) during the transition from the open to closed form (Scheme S19). In order to quantify the recovery rate constants k_b (s-1), we utilized a first order exponential recovery model $(k_{\text{b,exp'}}, \text{s}^{-1})^{24}$ and a dynamic equilibrium model $(k_{\text{b,dyn'}}, \text{s}^{-1})^{44,45}$ A detailed discussion on the two different kinetic models is summarized in Section 4 of the Supporting Information. For the kinetic studies, thin films were prepared by drop casting and irradiated with a light source (halogen lamp, EKE 150 W with a fiber optic illuminator, 172 mW/cm²) for 140 s at room temperature. In order to achieve an absorbance of ∼1, 1, 4, and 9 mol % DASA-based material thin films were prepared with different thicknesses of 10, 2.5, and 1 μ m, respectively, with the assumption that DASA has a molar extinction coefficient in the solid state similar to what has been experimentally determined in solution, ~100,000 M⁻¹ cm⁻¹.43,46

With increasing DASA content and increasing $T_{\rm g}$, we observed a slowing of the forward and backward reaction rates as shown in Figure 3a. The 1 mol % DASA–PHMA material with the lowest $T_{\rm g}$ has significantly more recovery at room temperature, at 71% of the initial absorbance, as compared to the 9 mol % DASA–PHMA material with the

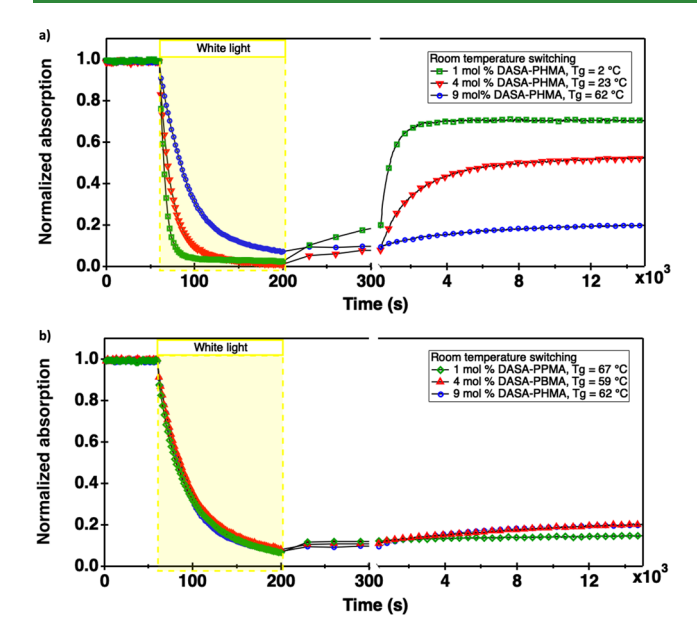


Figure 3. Influence of increasing DASA incorporation and T_g on the switching kinetics was determined using time-dependent pumpprobe UV/vis spectroscopy. Thin films were irradiated (halogen lamp, EKE 150 W with a fiber optic illuminator, 172 mW/cm²) starting at time t = 60 s and ending at t = 200 s (indicated by the shaded box in the time traces); the subsequent thermal recovery in the dark was measured. (a) Time-dependent UV/vis analysis of DASA-PHMA materials with $T_{\rm g}$ ranging from 2–62 °C due to increasing DASA incorporation. In a polymer matrix of fixed monomer composition, increasing DASA incorporation results in a decrease in the forward and backward reaction rates, as well as lower recovery. (b) Timedependent UV/vis analysis of materials with increasing DASA incorporation and different methacrylate comonomers resulting in materials with T_g ranging from 59–67 °C. In materials with a high T_g ≫ room temperature, and with similar initial absorbance, increasing DASA incorporation results in similar forward and backward reaction rates, and similarly low recovery.

highest T_{g} , which recovers only 20% after 15,000 s (>4 h). Analysis of the forward rate constants of 1, 4, and 9 mol % DASA-PHMA conjugates under illumination indicated a decrease in rate constants $(k_{\rm f,light}, {\rm s}^{-1})$ with increasing DASA content, 0.1350, 0.0660, and 0.0271 s⁻¹, respectively (Figure S19). While there is a slight variation between the two kinetic models for recovery, they are both in agreement that the rate constants decrease with increasing DASA incorporation and increasing $T_{\rm g}$ as summarized in Table S4. Overall, the lightdriven forward reaction rate dominates the kinetics, while the thermal back reaction rate occurs on a much slower time scale, which does not affect the macroscopic properties. We repeated the switching study with all DASA-PHMA materials at temperatures above their $T_{\rm g}$ using a heating bath that can reach a maximum sample temperature of 70 °C (for experimental details, see Section 5 in the Supporting Information). When each material is held over T_g , all materials recover to >70% as shown in Figure S23.

We then repeated these experiments for 1 mol % DASA–PPMA and 4 mol % DASA–PBMA materials that have T_g values of \sim 60 °C. As shown in Figure 3b, the three materials with similar T_g and initial absorbance all showed similar forward rate constants ($k_{\rm f,light}$, s⁻¹), with increasing DASA contents, 0.0271, 0.0244, and 0.0271 s⁻¹, respectively (Figure S22). In addition, both kinetic models indicated similar rate

constants for the thermal recovery of the materials bearing similar T_{g} regardless of DASA incorporation, as summarized in Table S4. The slight variation in recovery is likely due to the slight differences in T_g . At 70 °C, above the T_g of all three materials, there is a significant increase in thermal recovery, as shown in Figure S24. Consistent with the results obtained using the PHMA-based materials, recovery is roughly 70-80% regardless of the matrix and DASA incorporation when the operating temperature is held above $T_{\rm g}$. Additional studies are underway to better understand the 20-30% loss upon switching, which we believe may arise either because the material is reaching a new thermodynamic equilibrium or due to decomposition. Based on these results, it is clear that DASA incorporation and matrix selection dramatically influence the $T_{\rm g}$ of the material, which in turn dramatically influences the photoswitching properties.

Photothermal Actuation Performance. To demonstrate the effect of material design on light-driven actuation performance, we prepared bilayer actuators by drop casting DASA-based materials onto a commercially obtained polyimide (PI) film (purchased from McMaster, Kapton polyimide film, CTE $\sim 22.8 \pm 0.1 \times 10^{-6}$ and elastic modulus ~ 3.4 GPa at 1 Hz). The resulting material has a responsive DASAbased layer thickness of $\sim 10 \ \mu m$ and a passive layer thickness of \sim 25 μ m (Figure S25), and the planar sheet is cut into thin strips of 1.5 mm by 15 mm. Because stiffness increases by the cube of the thickness, all cantilevers are prepared with the same thickness of $\sim 10 \, \mu \text{m}$, regardless of mol % DASA incorporation. To evaluate the actuation performance of the different materials, a light source (halogen lamp, EKE 150 W with a fiber optic illuminator) located above the cantilever directly illuminated the DASA-PHMA layer. For each experiment, the displacement of the cantilever tip was continuously recorded before, during, and after irradiation, as shown in Figure 4a. An infrared camera (FLIR E60) was used to record the temperature of the bilayer cantilever under illumination. The actuation performance was measured under conditions of short- or long-term irradiation. Short-term irradiation is defined herein as ~4 s of irradiation time, resulting in negligible photoswitching in high T_g materials, as compared to long-term irradiation defined herein as >2 min of irradiation time, resulting in non-negligible photoswitching in all

To evaluate the short-term photothermal actuation of responsive bilayer materials, we initially measured cantilever tip displacement and temperature at different light intensities using the DASA-PHMA-coated materials with 1, 4, and 9 mol % incorporation of DASA (Figures 4b, S26a, and Table 1). At a given light intensity, we observed a slight temperature increase as the concentration of DASA increased. At the maximum light intensity of 172 mW/cm², for 1, 4, and 9 mol % DASA-PHMA conjugates, we measured 52.1, 57.9, and 62.4 °C, respectively. We attribute the slight variation in maximum measured temperature to (i) increasing DASA incorporation and (ii) the increased forward switching kinetics in lower T_g materials as shown in Figure 3a. The latter effectively lowers the percentage of the photothermal agent within the low $T_{\rm g}$ materials. The displacement versus measured temperature at different light intensities is summarized in Figure 4c. Here, we observed a significant increase in displacement as the concentration of DASA increases at a given light intensity. At the maximum light intensity of 172 mW/cm², a cantilever containing a 9 mol % DASA-PHMA active layer reached a

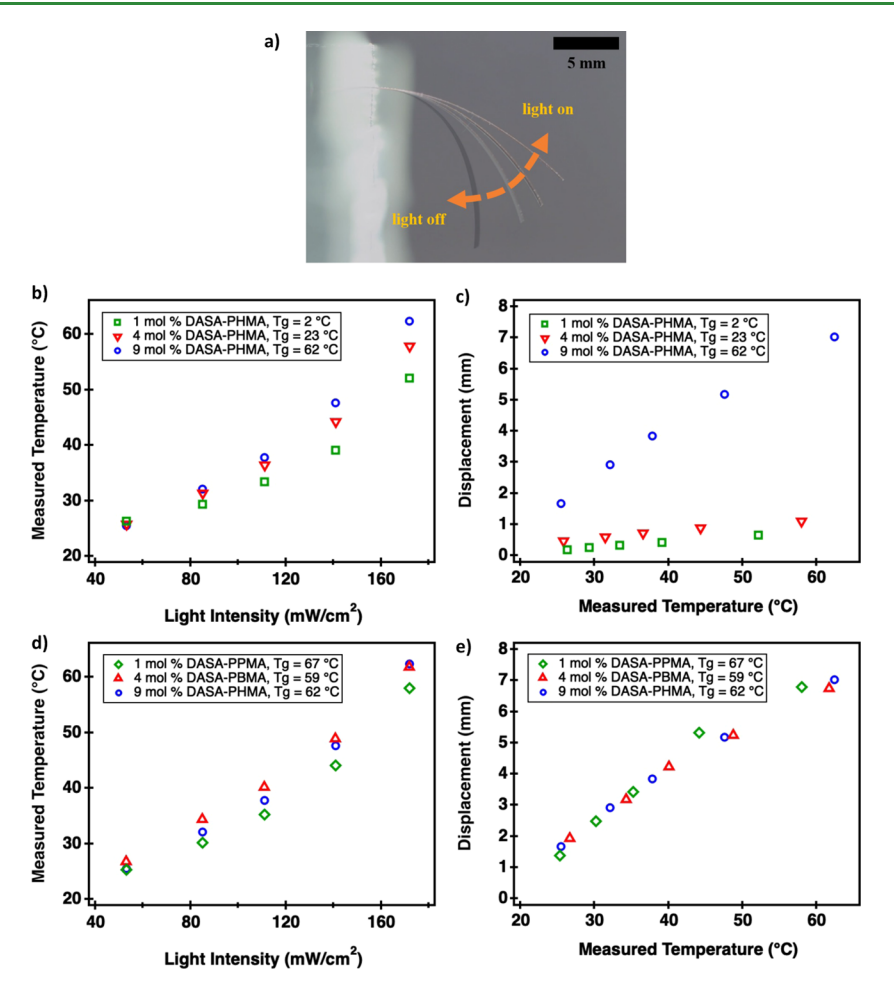


Figure 4. Photothermally driven actuation of DASA-based materials. (a) Using a cantilevered actuator geometry, we demonstrate the ability of the DASA-polymer to photothermally actuate upon irradiation with visible light. (b) Averaged peak temperature vs light intensity of DASA-PHMA materials with increasing DASA incorporation, resulting in a slight increase in temperature with increasing DASA incorporation. (c) Averaged peak displacement vs averaged measured temperature at different light intensities is plotted for DASA-PHMA materials, with significantly higher actuation for 9 mol % DASA-PHMA compared to lower incorporations. (d) Averaged peak temperature vs light intensity of DASA materials with increasing DASA incorporation and different methacrylate comonomers (PXMA). (e) Averaged peak displacement vs averaged measured temperature at different light intensities is plotted for DASA-PXMA materials, with similar actuation and temperature for all three materials. Averaged peak displacement is averaged over five total peak displacements and averaged peak temperature is averaged over three total measurements.

maximum deflection of 7.0 ± 0.1 mm and a temperature of 62.4 °C. Identical cantilevers containing 1 and 4 mol % DASA-PHMA demonstrated an approximate order-of-magnitude smaller displacement of 0.65 ± 0.06 and 1.11 ± 0.06 mm, respectively. We attribute the large difference in actuation performance to the differences in the stiffness of the materials, reflected in the $T_{\rm g}$ and modulus values. The 1 and 4 mol % DASA-PHMA materials have T_g at or below room temperature, and elastic moduli of 0.495 and 0.003 GPa at 20 °C, respectively. As a result, they do not provide enough bending stiffness to actuate the system. By contrast, the stiffer 9 mol % DASA-PHMA with a $T_{\rm g}$ = 62 °C significantly above room temperature, and elastic modulus = 1.608 GPa, outperforms the lower incorporation materials. While the role of the increasing concentration of the photothermal agent cannot be decoupled from the resulting change in mechanical properties among these three materials, it is clear that for a given passive bilayer, increasing the active layer stiffness improves actuation performance.

In order to decouple the changes in thermal and mechanical properties of DASA-based materials, we next tested the materials with differing comonomer compositions, thereby allowing us to increase the DASA incorporation without changing the $T_{
m g}$ or modulus values and evaluated their actuation performance in our cantilever device. Now, despite the significant differences in DASA incorporation, we measured very similar temperatures for all three materials, as shown in Figure 4d. Moreover, we observed similar displacements and temperatures at the same light intensities as the concentration of DASA increases (Figures 4e, S26b and Table 1). Initially, we were surprised by this result because one would anticipate that a higher concentration of the photothermal DASA agent would provide a better performance. However, this result is consistent with the Beer-Lambert law, where sample heating reaches an asymptotic limit when chromophore absorbance values are greater than $\sim 1.43,47$ Due to the high molar extinction coefficient of DASA ($\sim 100,000 \text{ M}^{-1} \text{ cm}^{-1}$), even at the lowest incorporation of 1 mol % DASA, the absorbance of the active layer has already reached this limit. Given that these materials have higher $T_{\rm g}$ values (~60 °C), they will have reduced forward photoswitching rates compared to the lower T_g materials. Together, these results establish that

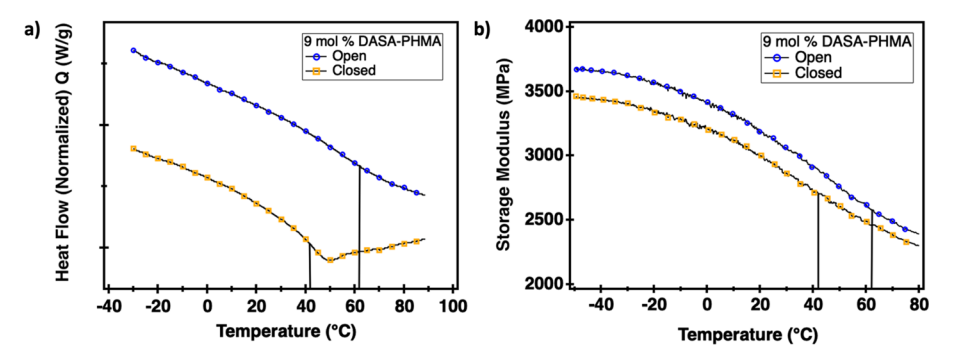


Figure 5. Photo-induced changes in mechanical properties between the open and closed-forms of DASA. (a) 9 mol % DASA–PHMA shows a significant drop in $T_{\rm g}$ upon switching observed by DSC. (b) A decrease in the elastic modulus between open and closed-form DASA at all temperatures is also observed using DMA. The vertical lines indicate the $T_{\rm g}$.

short-term actuation performance is not dependent on DASA incorporation in the range of 1–9 mol %, and that the actuation amplitude is primarily governed by the stiffness of the material as reported by the $T_{\rm g}$ and modulus.

Photo-Induced Material Property Changes. Unlike traditional photothermal agents or photoswitches, which absorb light in both states, DASAs are colorless and nonabsorbing in the switched state. This negative photochromism significantly impacts our photothermal material and provides a unique opportunity to leverage the properties of DASA in actuator design. To determine the relationship between actuation and photoswitching, we measured the long-term actuation performance. For these studies, we compared the 1 mol % DASA-PPMA, 4 mol % DASA-PBMA, and 9 mol % DASA-PHMA, all with high $T_{\rm g}$ values of ~60 °C and DASAlayer with a thickness of 10 μm (for experimental details, see Section 8 in the Supporting Information). Based on the studies of bleaching front propagation in solution, 43 we anticipate that the bleaching front propagates faster in the case of lower DASA incorporation, lowering the absorbance below the asymptotic limit more quickly than for the case of higher DASA incorporation. Experimentally, this was confirmed: as shown in Figure S27, the 1 mol % DASA-PPMA decreases in absorbance and maximum displacement more quickly than the 9 mol % DASA-PHMA. However, the 4 mol % DASA-PBMA and 9 mol % DASA-PHMA had a surprisingly similar long-term performance. Thus, while DASA incorporation does not govern the initial displacement obtained under short-term irradiation, it plays a role in how long the actuator has chemical energy (in the form of the light-absorbing species) to sustain the maximum (peak) performance.

The difference in performance under long irradiation times led us to also investigate the light-induced changes in mechanical properties between the photoreactant (openform) and photoproduct (closed-form), which we anticipate may arise from the large change in the molecular volume, 40 polarity, 25,46 and molecular interactions between the isomers. Using DSC, we determined the $T_{\rm g}$ of the closed-form 9 mol % DASA-PHMA using the first heating cycle. This contrasts our analysis of the open-form material, where three cooling cycles were analyzed, as subsequent heating cycles will thermally recover DASA to the open form as previously shown (experimental details are given in Section 9 of the Supporting Information). These results show there is a marked decrease in $T_{\rm g}$ of ~20 °C between the open (62 °C) and closed (42 °C) DASA forms, as shown in Figure 5a. The glass transition step is followed by a relaxation enthalpy due to the non-equilibrium

state. We suspect the decrease in $T_{\rm g}$ is due to the change in volume between the extended, open-form and the compact, closed-form. The photo-induced reduction in T_g is also supported by DMA as shown in Figure 5b. In addition, we observed a drop in the elastic modulus at 20 $^{\circ}\text{C}$ between the open- and closed-forms by DMA from 1.608 to 1.130 GPa, as measured by 1 Hz oscillation in the small strain regime as shown in Figure 5b (experimental details are in the Supporting Information in Sections 9 and 10). This suggests that the longterm actuation behavior is much more complex than a simple change in the absorbance/temperature change, and that there is a simultaneous and coupled change in material properties (modulus and T_g). To fully unlock the design potential of DASA-based materials, it is imperative to consider how these property changes may play a role in short- and long-term actuation performance, as well as the photoswitching reaction rates, which are highly dependent on these properties. To the best of our knowledge, this is the first example of photoinduced mechanical property changes of DASA-based materials. Such property changes have been observed in azobenzene-modified materials, although at near 100% photochrome incorporation.³⁹ The ability to access significant property changes at relatively low (9%) DASA incorporation shines light on the potential of DASAs to achieve more complex photo-induced property changes, in addition to their potential for applications in photoactuation.

CONCLUSIONS

Utilizing a modular Diels—Alder synthetic approach, we designed five materials, which systematically vary in DASA incorporation and glass transition temperature, as well as properties governing actuation performance such as elastic modulus. The results demonstrate important considerations for the design of application-geared DASA-materials, which address the trade-off of having a material that is stiff enough to actuate, but soft enough to reversibly switch at the operating temperature. Additionally, our results reveal light-induced property changes in the $T_{\rm g}$ and modulus between the open and closed forms of DASA-based materials. This work establishes the foundational relationships between mechanical and photoswitching properties and is critical to advancing the use of DASA-based materials.

ASSOCIATED CONTENT

Supporting Information

The Supporting Information is available free of charge at https://pubs.acs.org/doi/10.1021/acsapm.1c01108.

Experimental details; materials; characterization methods; optimized synthetic route to S1; glass transition temperature measurement by DSC; CTE for PI and DASA-based materials; DASA—PHMA thin film switching kinetics at room temperature; photoswitching of DASA-materials above $T_{\rm g}$; thickness measurement of 10 μ m using SEM; displacement vs. light intensity of DASA-based materials; long-term actuation of DASA-PXMA materials; $T_{\rm g}$ of closed-form 9 mol % DASA-PHMA (DMA and DSC); mechanical properties of closed-form 9 mol % DASA-PHMA (DMA); third-generation DASA used in this study; and 1 H and 13 C NMR spectra of polymer building blocks and DASA-based materials (PDF)

AUTHOR INFORMATION

Corresponding Authors

Megan T. Valentine — Department of Mechanical Engineering, University of California, Santa Barbara, California 93106, United States; orcid.org/0000-0003-4781-8478; Email: valentine@engineering.ucsb.edu

Javier Read de Alaniz — Department of Chemistry and Biochemistry, University of California, Santa Barbara, California 93106, United States; orcid.org/0000-0003-2770-9477; Email: javier@chem.ucsb.edu

Authors

Miranda M. Sroda – Department of Chemistry and Biochemistry, University of California, Santa Barbara, California 93106, United States

Jaejun Lee – Department of Polymer Science and Engineering, Pusan National University, Busan 46241, Republic of Korea Younghoon Kwon – Department of Mechanical Engineering, University of California, Santa Barbara, California 93106, United States

Friedrich Stricker – Department of Chemistry and Biochemistry, University of California, Santa Barbara, California 93106, United States

Minwook Park – Department of Chemistry and Biochemistry, University of California, Santa Barbara, California 93106, United States

Complete contact information is available at: https://pubs.acs.org/10.1021/acsapm.1c01108

Author Contributions

M.M.S. and J.L. contributed equally to this work. J.R.D.A. and M.T.V. jointly supervised the work.

Notes

The authors declare no competing financial interest.

■ ACKNOWLEDGMENTS

This work was primarily supported by the U.S. Army Research Office under Cooperative Agreement W911NF-19-2-0026 for the Institute for Collaborative Biotechnologies. Views and conclusions are those of the authors and should not be interpreted as representing official policies, either expressed or implied, of the U.S. Government. Support was also provided by the Office of Naval Research through the MURI on Photomechanical Material Systems through grant no. ONR N00014-18-1-2624 and National Science Foundation (NSF) through grant no. EFMA 1935327. M.M.S. was supported by the UCSB Graduate Opportunity Fellowship. Y.K. was supported by the

MRSEC Program of the National Science Foundation through grant no. DMR-1720256 (IRG-3). The authors acknowledge the use of the Microfluidics Laboratory within the California NanoSystems Institute, supported by the University of California, Santa Barbara and the University of California, Office of the President, and the MRL Shared Experimental Facilities supported by the MRSEC Program of the NSF under award no. DMR 1720256, a member of the NSF-funded Materials Research Facilities Network (www.mrfn.org). The authors thank Dr. Alexander Mikhailovsky for constructing the optical setup used for the switching experiment. The authors acknowledge the use of the Cornell Center for Materials Research Shared Facilities, which are supported through the NSF MRSEC program (DMR-1719875). The authors acknowledge the use of the NSF (grant no. MRI-1920299) for the acquisition of Bruker 500MHz and 400MHz NMR instruments.

REFERENCES

- (1) Kohlmeyer, R. R.; Chen, J. Wavelength-Selective, IR Light-Driven Hinges Based on Liquid Crystalline Elastomer Composites. *Angew. Chem., Int. Ed.* **2013**, *52*, 9234–9237.
- (2) Jiang, Z. C.; Xiao, Y. Y.; Yin, L.; Han, L.; Zhao, Y. "Self-Lockable" Liquid Crystalline Diels—Alder Dynamic Network Actuators with Room Temperature Programmability and Solution Reprocessability. *Angew. Chem., Int. Ed.* **2020**, *59*, 4925–4931.
- (3) Zuo, B.; Wang, M.; Lin, B. P.; Yang, H. Visible and Infrared Three-Wavelength Modulated Multi-Directional Actuators. *Nat. Commun.* **2019**, *10*, 1–11.
- (4) Verpaalen, R. C. P.; Pilz da Cunha, M.; Engels, T. A. P.; Debije, M. G.; Schenning, A. P. H. J. Liquid Crystal Networks on Thermoplastics: Reprogrammable Photo-Responsive Actuators. *Angew. Chem., Int. Ed.* **2020**, *59*, 4532–4536.
- (5) Pilz da Cunha, M.; Ambergen, S.; Debije, M. G.; Homburg, E. F. G. A.; den Toonder, J. M. J.; Schenning, A. P. H. J. A Soft Transporter Robot Fueled by Light. *Adv. Sci.* **2020**, *7*, 1902842.
- (6) Islam, M. R.; Li, X.; Smyth, K.; Serpe, M. J. Polymer-Based Muscle Expansion and Contraction. *Angew. Chem., Int. Ed.* **2013**, 52, 10330–10333.
- (7) Mirvakili, S. M.; Hunter, I. W. Artificial Muscles: Mechanisms, Applications, and Challenges. *Adv. Mater.* **2018**, *30*, 1704407.
- (8) Qian, X.; Chen, Q.; Yang, Y.; Xu, Y.; Li, Z.; Wang, Z.; Wu, Y.; Wei, Y.; Ji, Y. Untethered Recyclable Tubular Actuators with Versatile Locomotion for Soft Continuum Robots. *Adv. Mater.* **2018**, *30*, 1801103.
- (9) Lahikainen, M.; Zeng, H.; Priimagi, A. Reconfigurable Photoactuator through Synergistic Use of Photochemical and Photothermal Effects. *Nat. Commun.* **2018**, *9*, 1–8.
- (10) White, T. J.; Tabiryan, N. V.; Serak, S. V.; Hrozhyk, U. A.; Tondiglia, V. P.; Koerner, H.; Vaia, R. A.; Bunning, T. J. A High Frequency Photodriven Polymer Oscillator. *Soft Matter* **2008**, *4*, 1796–1798.
- (11) Gelebart, A. H.; Vantomme, G.; Meijer, E. W.; Broer, D. J. Mastering the Photothermal Effect in Liquid Crystal Networks: A General Approach for Self-Sustained Mechanical Oscillators. *Adv. Mater.* **2017**, *29*, 1606712.
- (12) Tang, Z.; Gao, Z.; Jia, S.; Wang, F.; Wang, Y. Graphene-Based Polymer Bilayers with Superior Light-Driven Properties for Remote Construction of 3D Structures. *Adv. Sci.* **2017**, *4*, 1600437.
- (13) Verpaalen, R. C. P.; Engels, T.; Schenning, A. P. H. J.; Debije, M. G. Stimuli-Responsive Shape Changing Commodity Polymer Composites and Bilayers. *ACS Appl. Mater. Interfaces* **2020**, *12*, 38829–38844.
- (14) Balani, K.; Verma, V.; Agarwal, A.; Narayan, R. *Physical, Thermal, and Mechanical Properties of Polymers*, 1st ed.; John Wiley & Sons, Inc., 2014.

- (15) Xie, R.; Weisen, A. R.; Lee, Y.; Aplan, M. A.; Fenton, A. M.; Masucci, A. E.; Kempe, F.; Sommer, M.; Pester, C. W.; Colby, R. H.; Gomez, E. D. Glass Transition Temperature from the Chemical Structure of Conjugated Polymers. *Nat. Commun.* 2020, 11, 1–8.
- (16) Jiang, W.; Niu, D.; Liu, H.; Wang, C.; Zhao, T.; Yin, L.; Shi, Y.; Chen, B.; Ding, Y.; Lu, B. Photoresponsive Soft-Robotic Platform: Biomimetic Fabrication and Remote Actuation. *Adv. Funct. Mater.* **2014**, *24*, 7598–7604.
- (17) Ma, H.; Hou, J.; Wang, X.; Zhang, J.; Yuan, Z.; Xiao, L.; Wei, Y.; Fan, S.; Jiang, K.; Liu, K. Flexible, All-Inorganic Actuators Based on Vanadium Dioxide and Carbon Nanotube Bimorphs. *Nano Lett.* **2017**, *17*, 421–428.
- (18) Lu, X.; Zhang, H.; Fei, G.; Yu, B.; Tong, X.; Xia, H.; Zhao, Y. Liquid-Crystalline Dynamic Networks Doped with Gold Nanorods Showing Enhanced Photocontrol of Actuation. *Adv. Mater.* **2018**, *30*, 1706597.
- (19) Kuenstler, A. S.; Kim, H.; Hayward, R. C. Liquid Crystal Elastomer Waveguide Actuators. *Adv. Mater.* **2019**, *31*, 1901216.
- (20) Livshits, M. Y.; Razgoniaev, A. O.; Arbulu, R. C.; Shin, J.; McCullough, B. J.; Qin, Y.; Ostrowski, A. D.; Rack, J. J. Generating Photonastic Work from Irradiated Dyes in Electrospun Nanofibrous Polymer Mats. ACS Appl. Mater. Interfaces 2018, 10, 37470–37477.
- (21) Ryabchun, A.; Li, Q.; Lancia, F.; Aprahamian, I.; Katsonis, N. Shape-Persistent Actuators from Hydrazone Photoswitches. *J. Am. Chem. Soc.* **2019**, *141*, 1196–1200.
- (22) Lancia, F.; Ryabchun, A.; Katsonis, N. Life-like motion driven by artificial molecular machines. *Nat. Rev. Chem.* **2019**, *3*, 536–551.
- (23) Lee, J.; Sroda, M. M.; Kwon, Y.; El-Arid, S.; Seshadri, S.; Gockowski, L. F.; Hawkes, E. W.; Valentine, M. T.; Read de Alaniz, J. Tunable Photothermal Actuation Enabled by Photoswitching of Donor-Acceptor Stenhouse Adducts. *ACS Appl. Mater. Interfaces* **2020**, *12*, 54075–54082.
- (24) Lui, B. F.; Tierce, N. T.; Tong, F.; Sroda, M. M.; Lu, H.; Read de Alaniz, J.; Bardeen, C. J. Unusual Concentration Dependence of the Photoisomerization Reaction in Donor-Acceptor Stenhouse Adducts. *Photochem. Photobiol. Sci.* **2019**, *18*, 1587–1595.
- (25) Sroda, M. M.; Stricker, F.; Peterson, J. A.; Bernal, A.; Read de Alaniz, J. Donor–Acceptor Stenhouse Adducts: Exploring the Effects of Ionic Character. *Chem. Eur. J.* **2021**, *27*, 4183–4190.
- (26) Sun, F.; Xiong, X.; Gao, A.; Duan, Y.; Mao, L.; Gu, L.; Wang, Z.; He, C.; Deng, X.; Zheng, Y.; Wang, D. Fast Photochromism in Solid: Microenvironment in Metal-Organic Frameworks Promotes the Isomerization of Donor-Acceptor Stenhouse Adducts. *Chem. Eng. J.* **2022**, *427*, 132037.
- (27) Lerch, M. M.; Wezenberg, S. J.; Szymanski, W.; Feringa, B. L. Unraveling the Photoswitching Mechanism in Donor-Acceptor Stenhouse Adducts. *J. Am. Chem. Soc.* **2016**, *138*, 6344–6347.
- (28) Lerch, M. M.; Di Donato, M.; Laurent, A. D.; Medved', M.; Iagatti, A.; Bussotti, L.; Lapini, A.; Buma, W. J.; Foggi, P.; Szymański, W.; Feringa, B. L. Solvent Effects on the Actinic Step of Donor—Acceptor Stenhouse Adduct Photoswitching. *Angew. Chem., Int. Ed.* **2018**, *57*, 8063–8068.
- (29) Zulfikri, H.; Koenis, M. A. J.; Lerch, M. M.; Di Donato, M.; Szymański, W.; Filippi, C.; Feringa, B. L.; Buma, W. J.; Di, M.; Szyma, W.; Filippi, C.; Feringa, B. L.; Buma, W. J. Taming the Complexity of Donor-Acceptor Stenhouse Adducts: Infrared Motion Pictures of the Complete Switching Pathway. *J. Am. Chem. Soc.* **2019**, *141*, 7376–7384.
- (30) Sanchez, D. M.; Raucci, U.; Ferreras, K. N.; Martínez, T. J. Putting Photomechanical Switches to Work: An Ab Initio Multiple Spawning Study of Donor-Acceptor Stenhouse Adducts. *J. Phys. Chem. Lett.* **2020**, *11*, 7901–7907.
- (31) Seshadri, S.; Bailey, S. J.; Zhao, L.; Fisher, J.; Sroda, M.; Chiu, M.; Stricker, F.; Valentine, M. T.; Read de Alaniz, J.; Helgeson, M. E. Influence of Polarity Change and Photophysical Effects on Photosurfactant-Driven Wetting. *Langmuir* **2021**, *37*, 9939–9951.
- (32) Ulrich, S.; Hemmer, J. R.; Page, Z. A.; Dolinski, N. D.; Rifaiegraham, O.; Bruns, N.; Hawker, C. J.; Boesel, L. F.; Read de Alaniz, J.

- Visible Light-Responsive DASA-Polymer Conjugates. ACS Macro Lett. **2017**, 6, 738–742.
- (33) Ulrich, S.; Wang, X.; Rottmar, M.; Rossi, R. M.; Nelson, B. J.; Bruns, N.; Müller, R.; Maniura-Weber, K.; Qin, X. H.; Boesel, L. F. Nano-3D-Printed Photochromic Micro-Objects. *Small* **2021**, *17*, 2101337.
- (34) Eisenbach, C. D. Effect of Polymer Matrix on the Cis-trans Isomerization of Azobenzene Residues in Bulk Polymers. *Makromol. Chem.* **1978**, *179*, 2489–2506.
- (35) Eisenbach, C. D. Cis-Trans Isomerization of Aromatic Azo Compounds Built in the Polyester Segment of Poly (Ester Urethanes). *Polym. Bull.* 1979, 1, 517–522.
- (36) Eisenbach, C. D. Investigation of Structure and Segmental Mobility of Poly(Ester Urethane)S By Using Photochromic Azobenzene Probes. J. Am. Chem. Soc. 1981, 21, 219–238.
- (37) Eisenbach, C. D. Isomerization of Aromatic Azo Chromophores in Poly(Ethyl Acrylate) Networks and Photomechanical Effect. *Polymer (Guildf)* **1980**, *21*, 1175–1179.
- (38) St. Amant, A. H.; Discekici, E. H.; Bailey, S. J.; Zayas, M. S.; Song, J.-A.; Shankel, S. L.; Nguyen, S. N.; Bates, M. W.; Anastasaki, A.; Hawker, C. J.; Read de Alaniz, J. Norbornadienes Robust and Scalable Building Blocks for Cascade "Click" Coupling of High Molecular Weight Polymers. J. Am. Chem. Soc. 2019, 141, 13619—13624.
- (39) Shin, J.; Sung, J.; Kang, M.; Xie, X.; Lee, B.; Lee, K. M.; White, T. J.; Leal, C.; Sottos, N. R.; Braun, P. V.; Cahill, D. G. Light-Triggered Thermal Conductivity Switching in Azobenzene Polymers. *Proc. Natl. Acad. Sci.* **2019**, *116*, 5973–5978.
- (40) Polymer Database: Poly(hexyl methacrylate). https://polymerdatabase.com/polymers/polyhexylmethacrylate.html (accessed Nov 2, 2021).
- (41) Hiemenz, P. C.; Lodge, T. P. Polymer Chemistry, 3rd ed.; CRC Press, 2020.
- (42) Strobl, G. R. The Physics of Polymers: Concepts for Understanding Their Structures and Behavior, 3rd ed.; Springer-Verlag Berlin Heidelberg, 2007.
- (43) Seshadri, S.; Gockowski, L. F.; Lee, J.; Sroda, M.; Helgeson, M. E.; Read de Alaniz, J.; Valentine, M. T. Self-Regulating Photochemical Rayleigh-Bénard Convection Using a Highly-Absorbing Organic Photoswitch. *Nat. Commun.* **2020**, *11*, 1–8.
- (44) Hemmer, J. R.; Poelma, S. O.; Treat, N.; Page, Z. A.; Dolinski, N. D.; Diaz, Y. J.; Tomlinson, W.; Clark, K. D.; Hooper, J. P.; Hawker, C.; Read de Alaniz, J. Tunable Visible and Near Infrared Photoswitches. *J. Am. Chem. Soc.* **2016**, *138*, 13960–13966.
- (45) Dolinski, N. D.; Page, Z. A.; Eisenreich, F.; Niu, J.; Hecht, S.; Read de Alaniz, J.; Hawker, C. J. A Versatile Approach for In Situ Monitoring of Photoswitches and Photopolymerizations. *ChemPhotoChem* **2017**, *1*, 125–131.
- (46) Helmy, S.; Leibfarth, F. A.; Oh, S.; Poelma, J. E.; Hawker, C. J.; Read de Alaniz, J. Photoswitching Using Visible Light: A New Class of Organic Photochromic Molecules. *J. Am. Chem. Soc.* **2014**, *136*, 8169–8172.
- (47) Spence, G. T.; Hartland, G. V.; Smith, B. D. Activated Photothermal Heating Using Croconaine Dyes. *Chem. Sci.* **2013**, *4*, 4240–4244.